CHAPTER 2

THE DECAMETER-WAVE RADIO-TELESCOPE AT GAURIBIDANUR AND THE NEW TRACKING SYSTEM

2.1 INTRODUCTION

In order to make sensitive observations of pulsar signals at low radio-frequencies a suitable radio-telescope with large collecting area is essential. The decameter-wave radio-telescope at Gauribidanur, India, built and used for continuum observations, could be used for pulsar observations only after suitable improvements. In the first section of this chapter, a brief description of the telescope system is given, as it existed before pulsar observations were taken up. The capabilities of this system in the context of pulsar observations are discussed in the next section. In the last section, a detailed account of a new tracking facility built for improving the sensitivity of the telescope by a factor of about 5, which is essential for pulsar observations with this telescope, is presented.

2.2 THE DECAMETER-WAVE RADIO-TELESCOPE AT GAURIBIDANUR

2.2.1 The Antenna System

The low frequency Radio-Telescope at Gauribidanur, operating at 34.5 MHz, is a meridian transit instrument. The telescope consists of 1,000 broad band dipoles arranged in a form of the letter "T". A schematic of the dipole is shown in Fig. 2.1 . The outputs of four such dipoles along the East-West direction are combined in Christmas tree fashion using open wire (balanced) transmission lines, transformers and a BALUN (BALanced to UNbalanced transformer) to form a "basic element" as shown in Fig. 2.2 . Such basic elements, numbering two hundred and fifty, are arranged to form a 1.38 Km long "EW" array along the East-West direction and a 0.45 Km long "S" array extending southwards from the centre of the EW array as shown in Fig. 2.3 .

The EW array consists of ten groups of sixteen basic elements each. In each of such groups, the 16 basic elements are arranged in the form of 4 x 4 matrix. The outputs of the basic elements are combined as shown in Fig. 2.4a to produce a "group" output. Five group outputs, available from each of the East and West arms, are combined separately with equal delay and amplitude in the form of a Christmas tree. The East and West arm outputs are amplified and are brought to the

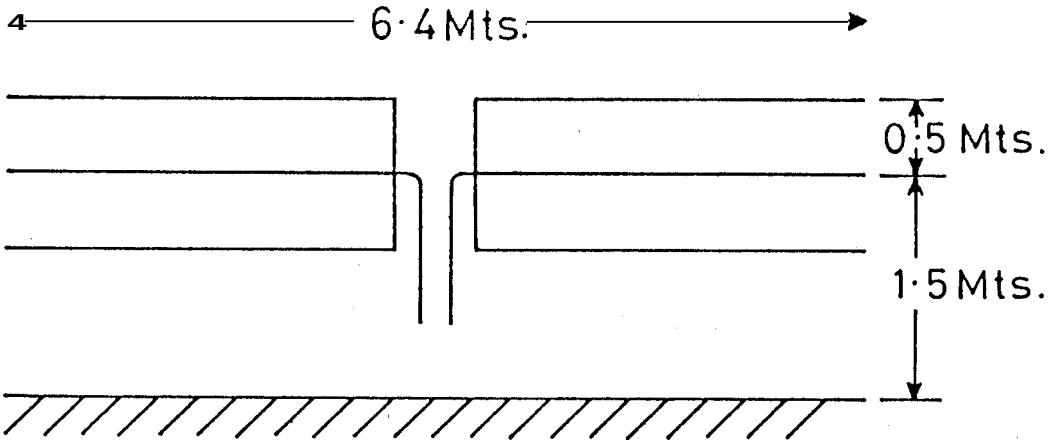

Imedance → 600Ω , V. S.W. R → 1·1 to 1.5
Bandwidth → 10 MHz around 32 MHz
Polarization → linear in E-W direction

FIG. 21 Schematic of the dipole.

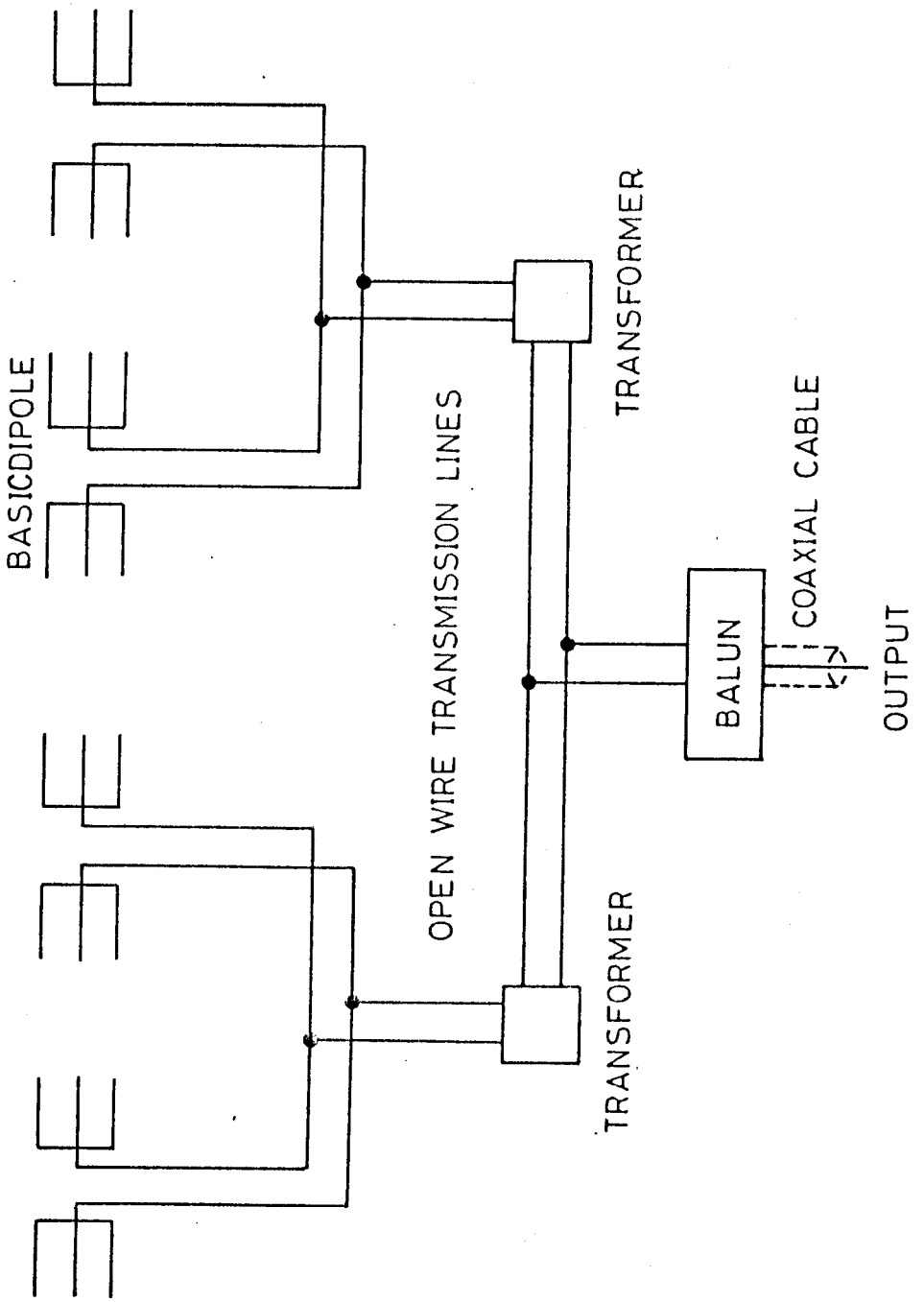

FIG.2.2 The basic array element.

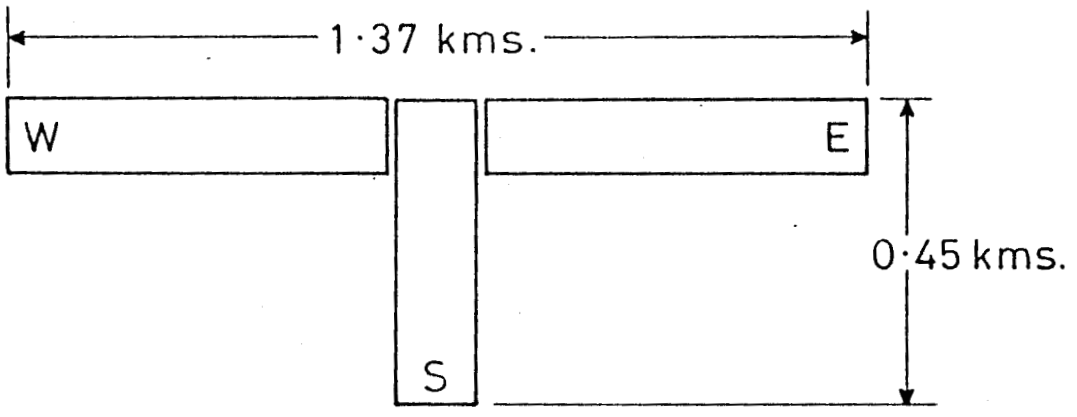

1. Instrumental zenith → 14°.1 N
2. EW ARRAY *4* rows of *40* basic elements each
3. S ARRAY *90* rows of one basic elements each
4. SPACING 34.4 mts. in E-W direction
   5 mts. in N-S direction

FIG.2.3 The "T" array at Gauribidanur

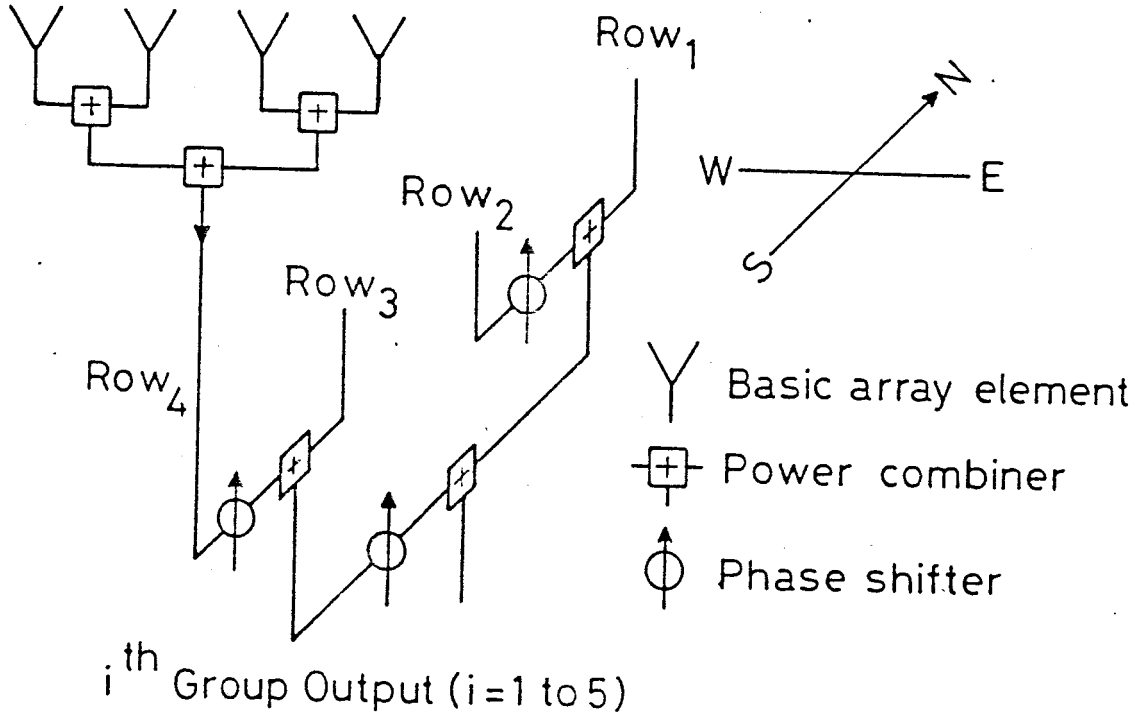

Fig. 2.4a CONFIGURATION WITHIN EACH EW GROUP

receiver room (see Fig. 2.4b).

The S array consists of ninety basic elements arranged along the N-S direction. The output of each element is amplified using a FET pre-amplifier. These amplified outputs are' then combined together in Christmas tree fashion using diode phase shifters, power combiners and amplifiers at appropriate stages as shown in Fig. 2.5 . This final output is brought to the receiver room.

Under ideal conditions, the voltage beam patterns, of the EW and S array in the E-W and N-S directions, can be described by SINC (i.e. SIN(x)/x) functions. These beams can be tilted in the N-S direction by setting appropriate phase gradients along the N-S direction with the help of the diode phase shifters used in the feeder system. A special purpose control system is used to generate appropriate control signals for these phase shifters.

The antenna outputs, EW and S, can be used in many different operating modes. The possible operating modes, along with the corresponding beam widths and the effective areas are listed in Table 2.1 .

2.2.2 Receiver Systems

The existing telescope includes two different kinds of receiver systems, namely, a single frequency-channel analog

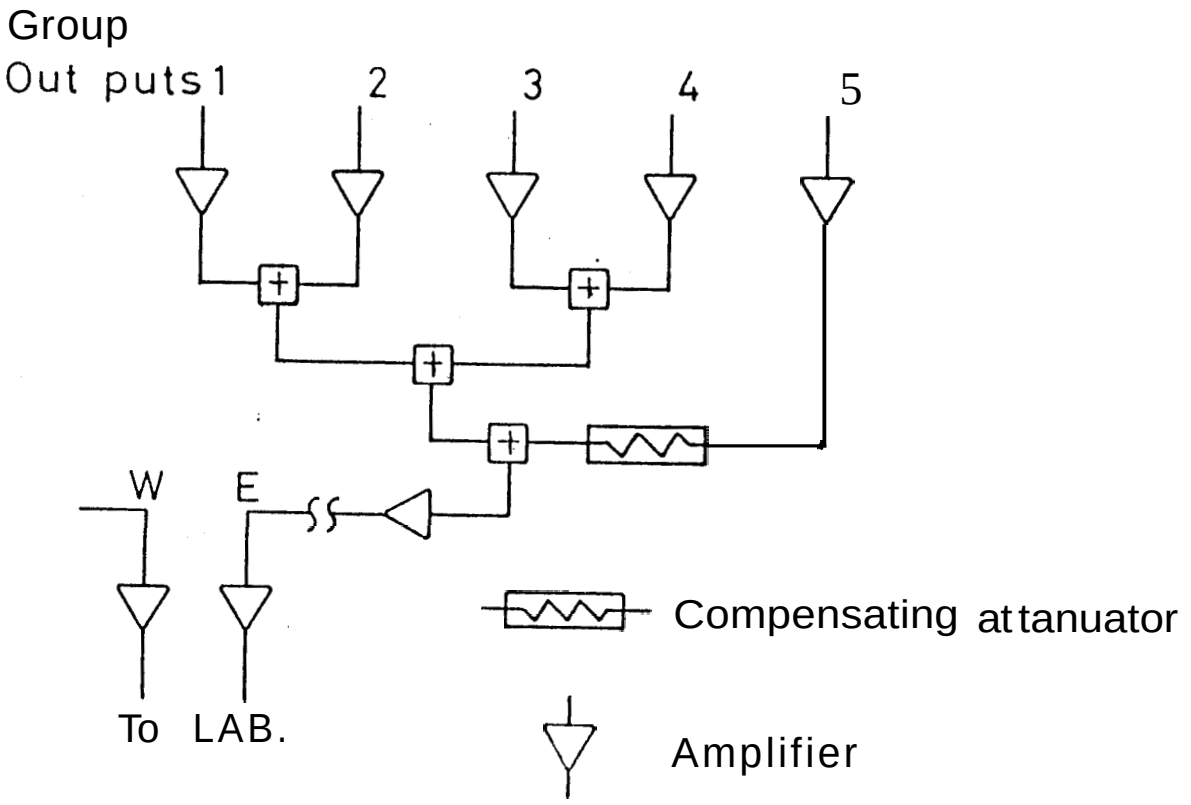

Flg. 2.4b Combination of the groups in the EW array.

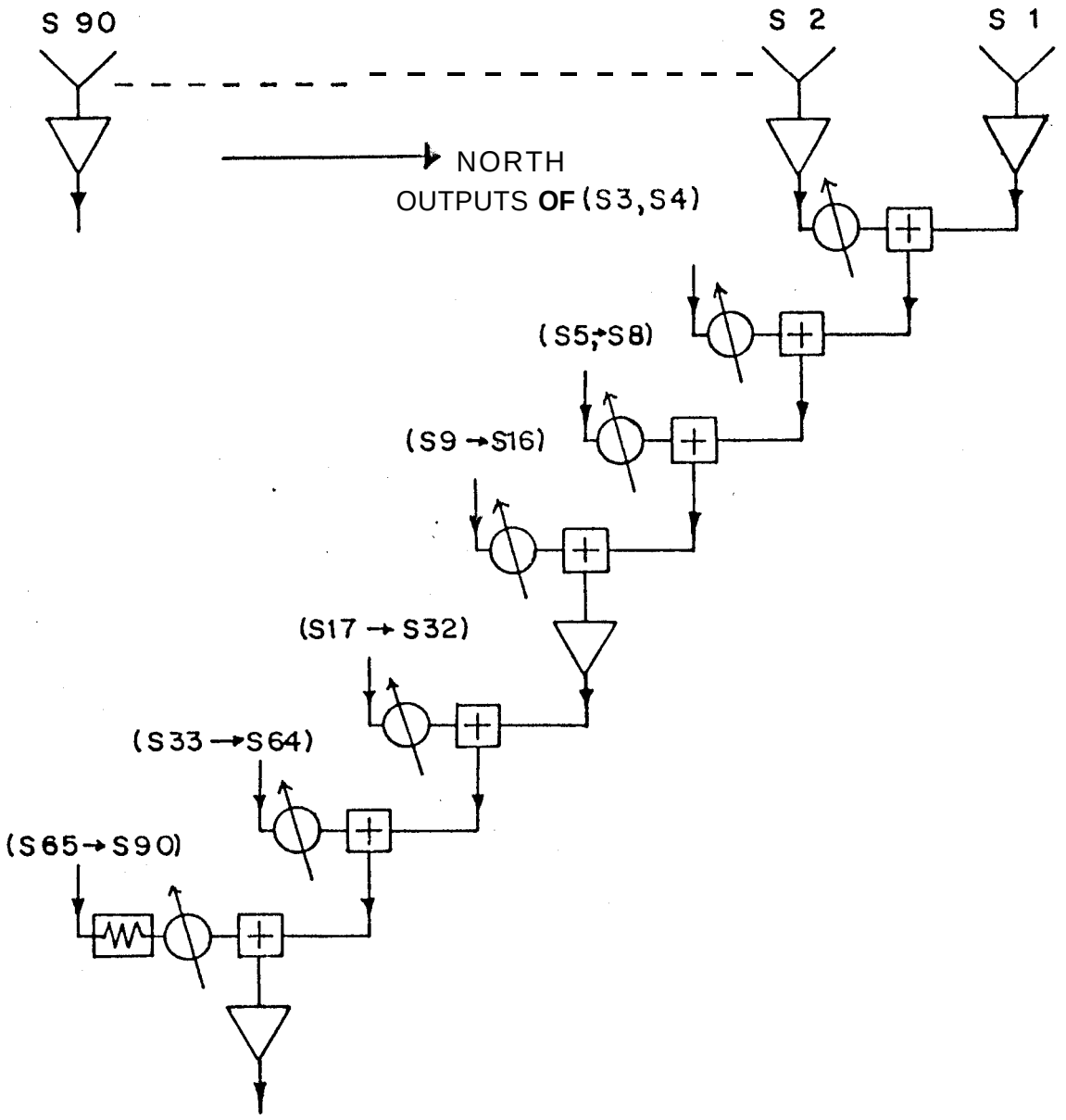

FIG.2.5 Configuration in the south array.

Operating mode	Beam width @ (RA x DEC)	Effective collecting area (Ae) at zenith
$(E+W)^2$, Total power	21' x 25°	160 λ^2
(E+W)xS, Correlation	26' x 40'	240 λ^2
S^2, Total power	14°.5 x 69'	90 λ^2
$(E+W+S)^2$, Total power	*	250 λ^2

@ full width at half power points at zenith

* Refer to section 4.5 .

TABLE 2.1 OPERATING MODES OF THE GAURIBIDANUR TELESCOPE WITH THE CORRESPONDING BEAM WIDTHS AND EFFECTIVE COLLECTING AREA.

correlation receiver and a 128 channel digital correlation receiver.

The analog receiver can be used to realize any one of the different modes described in Table 2.1 . A simplified block diagram of this receiver is shown in Fig. 2.6 . The RF inputs A and B are amplified and down converted to an intermediate frequency (IF) of 11.5 MHz. Using appropriate IF filters, the receiver predetection bandwidth can be selected from the three possible bandwidths, namely 30 KHz, 200 KHz and 1 MHz. Two independent correlations, namely the inphase (COS) and the quadrature (SIN), are obtained at the output of the receiver. The post-detection gain and the integration time-constant can be suitably selected. The data thus obtained can be recorded only in the analog form using chart recorders.

Typically, the inputs A and B are the EW and the S array outputs. In such a case, the outputs of the receiver (i.e. COS and SIN correlations) are proportional to the voltage gains of the two independent beams produced in the N-S direction. Both the outputs as a function of time, in an ideal situation and in the case of a point source, represent the voltage beam response of the EW array in the E-W direction. This receiver can also be used as a "total power receiver" by feeding the same signals to both A and B ports.

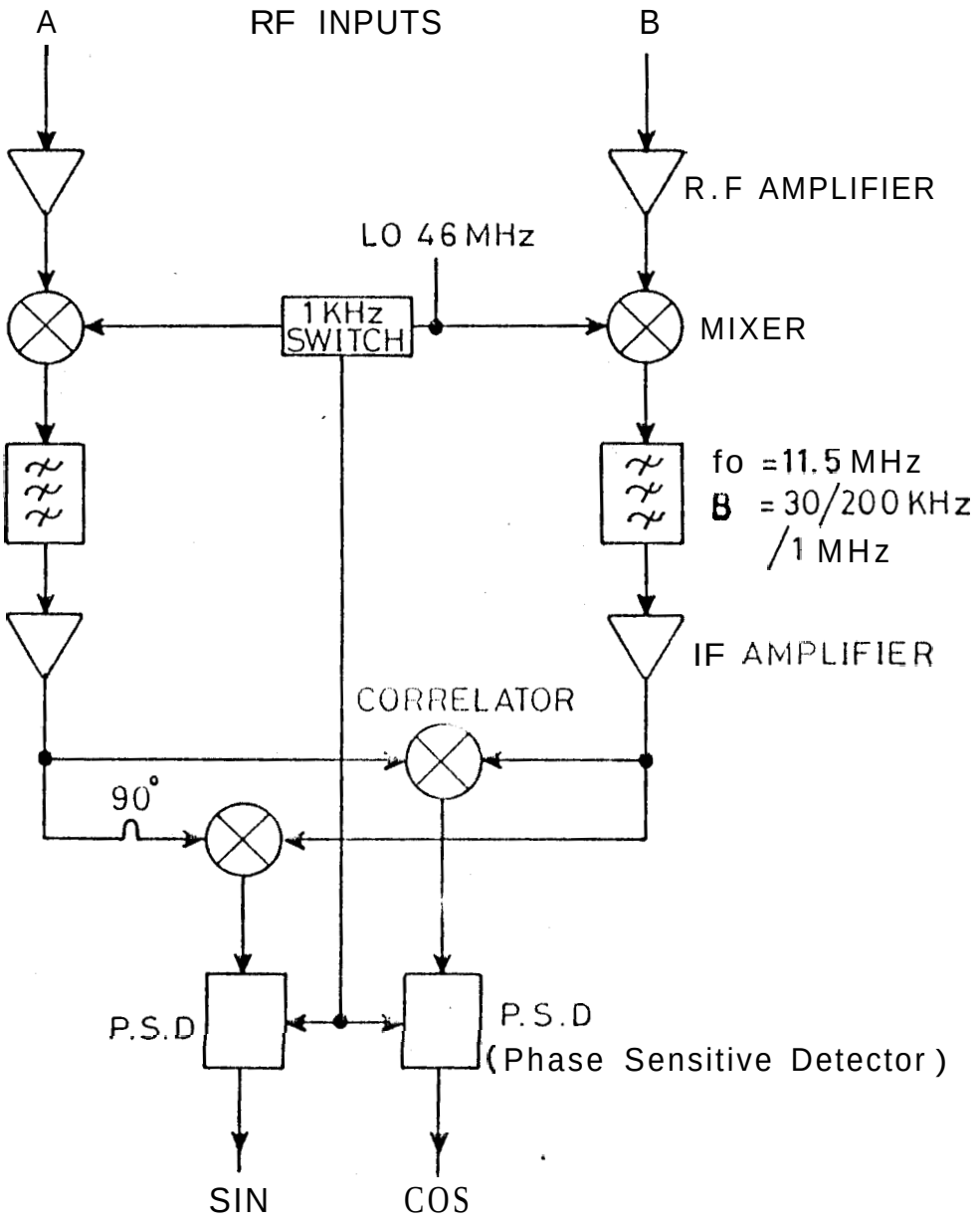

FIG. 2.6 Block diagiam of the analog receiver.

The 128 channel digital correlation receiver was built, and has been used successfully, for continuum mapping and spectral line observations (Udayashankar,1986) [87]. In the continuum mode, it is used for one dimensional aperture synthesis observations. In the spectral line mode, the receiver uses the "Autocorrelation method" based on the Wiener-Khinchin theorem which states that the power spectrum and the autocorrelation function of a signal form a Fourier transform pair. Since only the latter mode is relevant to the present work, we refer to the receiver as the "Autocorrelation receiver". This receiver accepts only one input signal whose autocorrelation in the time domain is to be measured. A simplified block diagram of this receiver is shown in Fig. 2.7 . The front end is a conventional double sideband (DSB) receiver. The low-pass filters are used to band limit the two side band contributions symmetrically. The filtered singals are zero-cross detected and sampled to produce one-bit outputs. One-bit correlators are used with shift registers to produce complex autocorrelations for 0 to 127 delay steps. The delay step is equal to the inverse of the sampling frequency. The sampling is normally done at the Nyquist rate. The low-pass filters have sharp cutoffs in order to avoid aliasing. The correlations thus obtained are recorded on magnetic tape. Later, these one-bit correlations are converted to analog correlations, using the Van-Vlack relation [88],and are Fourier transformed using a computer. This kind

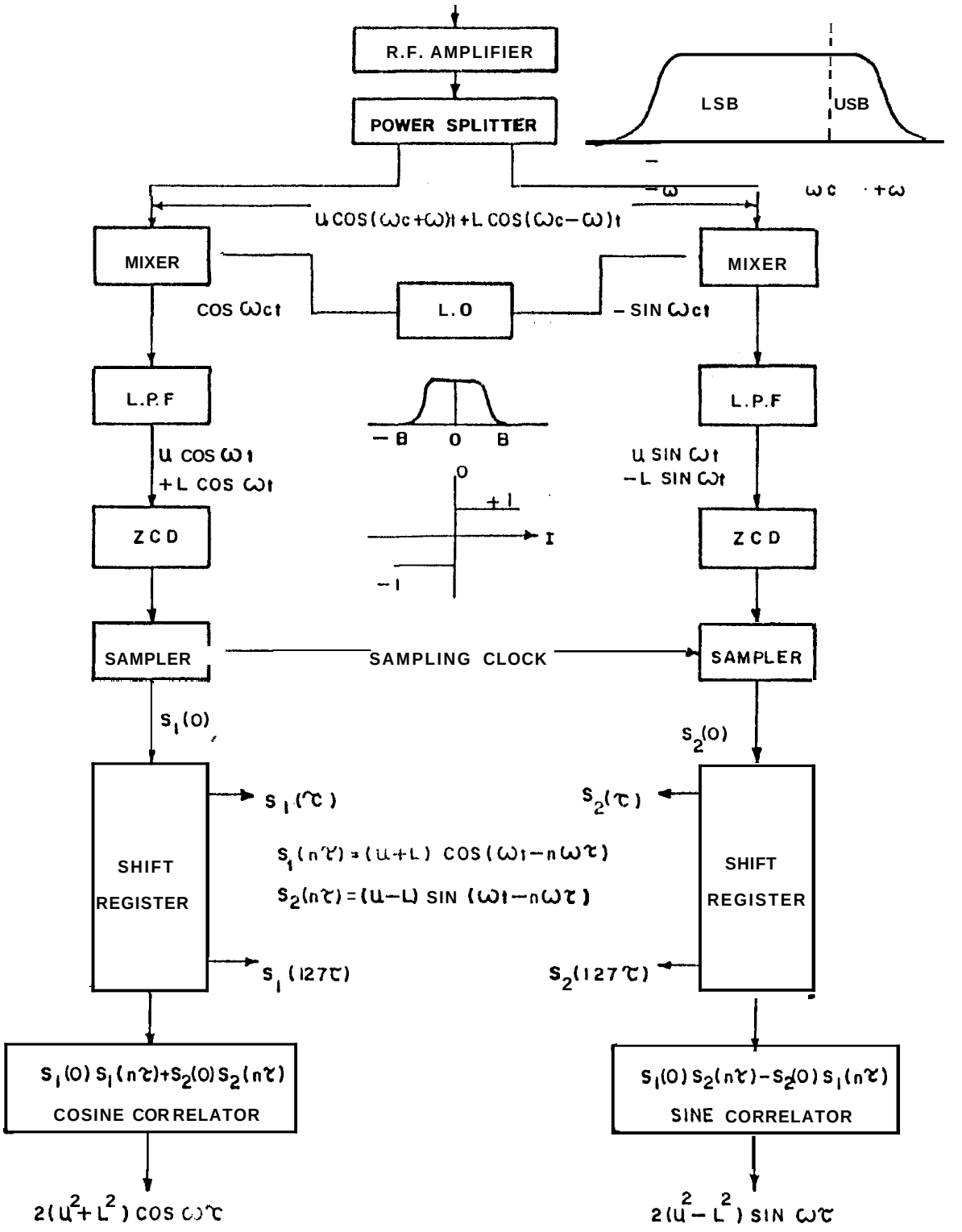

FIG.2.7 Block diagram of the Autocorrelation Receiver.

(Udayashankar, 1986)(87)

of a receiver is superior to a filter channel receiver because of its stability and flexibility for obtaining different frequency resolution. However, it should be noted, that one-bit processing has some disadvantages. Firstly, when the Nyquist sampling rate is used, the signal-to-noise ratio is reduced to 67% of that obtainable in analog processing under otherwise identical conditions. Secondly, due to the normalized nature of the one-bit correlations, the absolute amplitude information is lost. The amplitude information can be recovered, however, by measuring the total power of the signal before the zero-cross detection.

2.3 SYSTEM CAPABILITIES

The Gauribidanur telescope is essentially a meridian transit instrument. When the outputs of the EW and S arms are correlated in phase, a pencil beam of half power width **26'** X 40'SEC(Z) arc is obtained, where Z is the zenith angle. This correlation team can be pointed to any direction along the meridian within a declination range of -45° to+75° in steps of 12' arc. The ideal beam patterns in the E-W and **N-S** direction, cqrresponding to the COS correlation, are close to **SINC** functions. Because the beamwidth in the E-W direction is 26' arc, a point source can be observed for only about 2.SEC(δ) minutes in a day, where δ is the declination of the source.

The sensitivity of a radio telescope, expressed in terms of the minimum point source flux that can be detected, ΔS_{min}, is defined [89] as

$$\Delta S_{min} = \frac{Q\, m'(2k\, T_{sys})}{A_e \sqrt{(B\, \tau\, n_{samp})}} \qquad .....(2.1)$$

where, Q = a factor by which the ΔS_{min} should be larger than the r.m.s. deviations due to noise

m' = Receiver dependent constant. ≥ 1

k = Boltzman's constant
$= 1.38 \times 10^{-23}$ W Hz^{-1} K^{-1}

Tsys = System noise temperature.

Ae = Effective aperture size.

B = Predetection bandwidth.

τ = Post-detection integration time.

n_{samp} = Number of independent samples averaged after post-detection integration.

The value of Q determines the level of significance for detection. We use Q=5 for the present purpose. The receiver dependsnt cosntant, m', is equal to 1.41 [90] in the case of the analog correlation receiver described earlier. The system noise temperature is the sum of the antenna and the receiver noise temperatures [89]. At decametric wavelengths, due to

the bright sky background [73], the antenna temperture is very high compared to the receiver noise temperature. Therefore the system temperature can effectively be assumed to be equal to the sky background temperature. The system temperature and therefore the sensitivity varies by a factor of ~ 4 depending upon which part of the sky is observed. The effective aperture size in the correlation mode (see Table 2.1) is equal to $240\,\lambda^2\,\cos(Z)$ sq. meters, where Z is the zenith angle and λ is the wavelength of observation.

As the values for Tsys, Ae and m' are more or less fixed for the existing system at Gauribidanur, the sensitivity now depends on the choice of B, τ and n_{samp}. In the case of continuum observations, B can be increased to as high as 1 MHz, while τ can be as high as 25 sec. Assuming $n_{samp}=1$ and Tsys= 20,000 K, the minimum detectable flux for the continuum observation in correlation mode is ~ 0.5 Jansky (where 1 Jansky= 10^{-26} W m^{-2} Hz^{-1}).

However, the sensitivity obtainable in one day for pulsar observations is more limited due to the rollowing factors.

1) The choice of predetection bandwidth, B is very much restricted to quite low values due to the dispersion of pulsar signals in the interstellar medium. The optimum bandwidth [91], for maximum signal-to noise ratio in such a case, is the bandwidth over which the dispersion smearing is equal to the

undispersed pulse width.

This bandwidth at 34.5 MHz is given by

$$B_{opt} = 5.W/DM \quad MHz \qquad .....(2.2)$$

where W = Undispersed pulse width in seconds

DM = Dispersion measure.

Assuming DM = 10 $cm^{-3}pc$ and W = 0.05 sec, we find that Bopt = 25 KHz.

2) The post-detection time constant, τ , should be small compared to the width of at least the dispersed pulse in order to avoid additional smearing.

3) The number of independent samples at each longitude (see Appendix III for definition) of a pulsar signal is equal' to the number of pulses received during one transit observation, if a single frequency channel receiver is used. As observation of a pulsar at a declination δ is possible over a duration of 2 SEC(δ) minutes in one day, the effective number of independent samples is given by

$$n_{samp} = 120.d'.SEC(\delta)/P \qquad .....(2.3)$$

where P = pulsar period in seconds.

and d' = a constant to account for the average gain of the EW beam over 30' arc.

Keeping in mind the above cosntraints, the minimum detectable

peak flux for pulsars is about 15 Jansky (assuming n_{samp}=100, τ=100 milliseconds and B=25 KHz). This sensitivity is too poor to detect even the strongest of the pulsars at 34.5 MHz.

The number of independent samples could be increased by increasing the observing time if we use the south arm in the total power mode, because of the large beamwidth of this arm in the E-W direction. However, the effective collecting area in this case would much less than the effective collecting area in the correlation mode. Therefore, the final sensitivity improvement could not be more than a factor of ~ 2. It is clear that the telescope in the transit mode is not adequate for pulsar observations. To improve the sensitivity of the telescope, a tracking system was built so that observations are possible over a longer period with the maximum possible collecting area of the "T" array. In the next section, we discuss the design of this tracking system in detail.

2.4 THE TRACKING SYSTEM

2.4.1 Basic Scheme

The amount of time over which a point source can be observed, can be increased by tracking the source as it moves from East to West for an observer on the Earth. In the

existing meridian-transit telescope system, the antenna beam can be electronically steered to a given declination along the meridian using the existing phase shifters. In the E-W direction the basic array elements are combined with equal phases and amplitudes. Thus the antenna response in the E-W direction is maximum at the meridian. While the EW arm of the "T" antenna has a narrow response in the E-W direction, the south arm has a much wider response in that direction. If the EW beam of the EW array can be tilted sequentially within the E-W beam of the south arm, it is possible to obtain the required increase in the observing time. Thus, we can achieve the required tracking by introducing appropriate delay gradients in the EW array alone.

In order to introduce the required delay gradients in the EW array, we need to introduce a large number of delay shifter modules in the existing feeder system. These modules should ideally be introduced at the output of each dipole in the EW array. But it suffices to introduce them at the outputs of the basic elements, considering that the response of the basic element in the E-W direction is similar to that of the south array. Thus the number of required delay shifters and the complexity of this system can be reduced. However, the price for this simplification is paid in terms of the appearence of unwanted "secondary" (Grating) responses. Although the grating response may not have very serious effects in the case

of pulsar observations, it is of concern for the following reasons. Firstly, the gain of the primary response reduces when tilted away from the meridian, as both primary and secondary responses are weighted by the EW power response of the basic elements, i.e. by a function $\mathrm{SINC}^2(\pi\theta_m/\theta_b)$. Secondly, the grating response can cause confusing contributions from unwanted directions in the case of other kinds of observations (e.g. scintillation observations). It can be shown, that the ratio $R_g(\theta_m)$ of the secondary response to the main response is given by

$$R_g(\theta_m) = \left[\frac{\mathrm{SINC}\,[\,\pi(1-\theta_m/\theta_b)\,]}{\mathrm{SINC}\,[\,\pi(\theta_m/\theta_b)\,]} \right]^4 \qquad .....(2.4)$$

where $\mathrm{SINC}(x) = \sin x/x$

θ_m = Angular tilt from the meridian.

θ_b = Angular seperation between the peak and the first null of the EW response of the basic element.

This ratio increases with θ_m. Therefore, the value of the maximum angle (θ_{max}), to which the EW beam can be tilted away from the meridian, needs to be optimized with respect to the grating response. We have chosen a value for θ_{max} of about 5°, such that the grating response contribution on the average is less than 10% of the contribution due to the main

response and the value of $R_g(\theta max)$ is about 0.25.

The angular step by which the sequential EW beams should be separated is chosen to be 10' arc, such that the sequential beams overlap at 95% gain points of the correlation beams. Smaller values of the angular step are not advantageous considering the subsequent increase in the number of sequential beams and the complexity of the system.

Ideally, we need to set a delay gradient along the array. The maximum possible value of the delay that should be compensated for in this case is

$$\tau max = L_{EW}.SIN(\theta max)/c \qquad .....(2.5)$$

where L_{EW} = length of the EW array

c = velocity of light

If we compensate for the phases instead of the delays, it will result in decorrelntion over the system bandwidth B. This decorrelation factor is given by [92]

$$\eta = SINC(\pi B \bar{\tau}) \qquad .....(2.6)$$

where $\bar{\tau}$ = the mean uncompensated delay.

In our case, the maximum value of η is ~ 0.93, assuming B=1 MHz and $\tau = \tau_{max}/2$. Therefore, we can neglect this effect of small decorrelation and afford not to compensate for the delays.

Thus, by introducing 63 phase gradients sequentially along the E-W direction in the EW array alone, it is possible to track a source over a total span of $10^{\circ}.5$ centered around the meridian. This corresponds to $42.SEC(\delta)$ minutes of observing time for a source at a declination δ. With this basic idea, we will now consider some important aspects of the linear phase gradients required to be introduced in the EW array.

Firstly, we do not want to disturb the phase centre of the EW array which is at the physical centre of the array. Therefore any phase gradient introduced along the E-W direction should have zero phase contribution at the centre of the EW array. This means that there will be an inverse symmetry between the phases to be introduced in the E and W arrays with respect to the centre. This inverse symmetry can be used to our advantage, so that only those values of the phases required for a gradient to be set over the East arm need to be generated. The corresponding values of the phases to be used in the West arm can he then obtained by just changing the sign of those for the East arm. Further, any two beam positions placed symmetrically about the merdian need

their corresponding phase gradients to be equal but opposite in sign. This aspect also can be made use of to simplify things further. Thus all values of the phase gradient, across the EW array required to obtain the 63 beam positions, can be extracted from the knowledge of the 32 phase gradients needed for the E arm of the EW array. It can be shown, that the phase gradient, $Ge(\theta_m)=(d\phi/dl)east$, to be set along the E arm for tilting the beam by an angle θ_m towards East of the meridian, can be written as

$$Ge(\theta_m) = -2\pi.SIN(\theta_m)/\lambda \quad \text{radian/meter} \quad .....(2.7)$$

where λ = wavelength of operation in meters.

Following the discussion above, we can now write

$$\begin{aligned} Gw(\theta_m) &= -Ge(\theta_m) \\ &= Ge(-\theta_m) \\ &= -Gw(-\theta_m) \end{aligned} \qquad .....(2.8)$$

where Ge, Gw are defined with respect to the centre of the EW array.

The maximum value for the phase gradient is then

$$\begin{aligned} |G|max &= 2\pi SIN(\theta max)/\lambda \\ &= 3^{\circ}.8 \quad /meter \end{aligned} \qquad .....(2.9)$$

In order to set the required phase gradients, we need to introduce remotely controlled phase shifters in the existing feeder system of the EW array. If a phase shifter is

introduced at the output of each basic element, we would need to generate, and transmit to the field, 40 independent sets of control signals for the phase shifters. But if these phase shifters are introduced by making use of the already existing Christmas tree connections as shown in Fig. 2.8a,b , only 10 sets of control signals will be required. Also, as the four rows along the N-S direction are combined within each group, the number of phase shifter modules needed will be reduced to 120 from 160 in the earlier case. As shown in the Fig, 2.8a, 4 basic elements in each of the four rows of a group can be combined with phase shifts $\phi 1$ and $\phi 2$. The four rows in esch group are combined with the already existing declination phase shifters to produce a group output. Five such group outputs in each of the E and W arms can then be combined using phase shifts $\phi 3$, $\phi 4$ and $\phi 5$ (Fig. 2.8b).

It should be noted that the existing aperture of the EW array has a hole at its centre Fig. 2.9a . For simplicity, we can introduce the required phase slopes along the E and W arms such that the basic elements closest to the centre on either side get no phase shift as shown in Fig. 2.9b . But in such a case, the phases across the E and W arms will have equal and opposite phase offsets compared to the required phases (Fig. 2.9c). This offset phase happens to be equal to the phase difference ($\phi 1$) to be introduced between two adjecent basic elements on respective sides. The final outputs of E

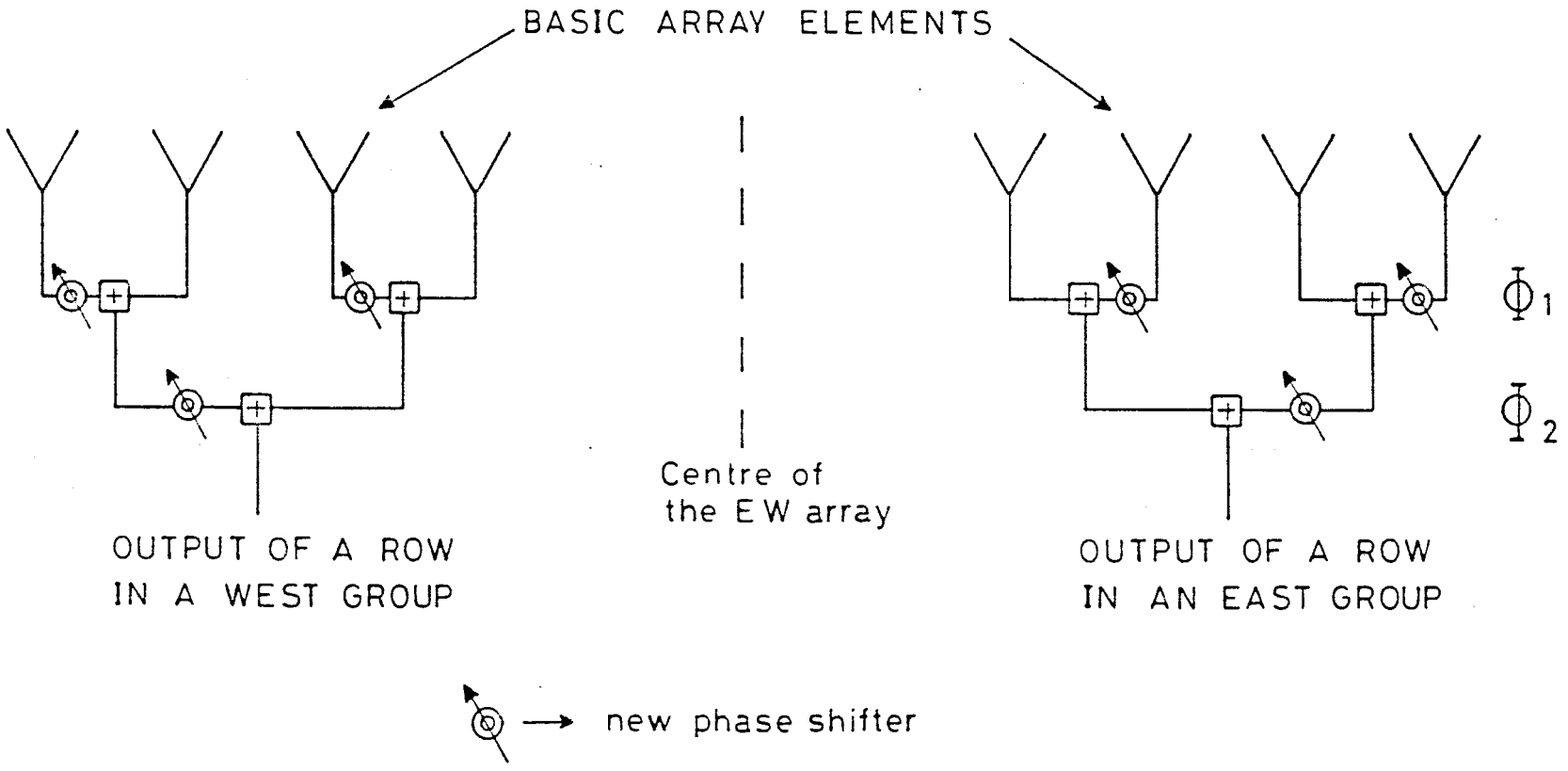

Fig.2.8a INTRODUCTION OF NEW PHASE SHIFTER $\Phi 1, \Phi 2$

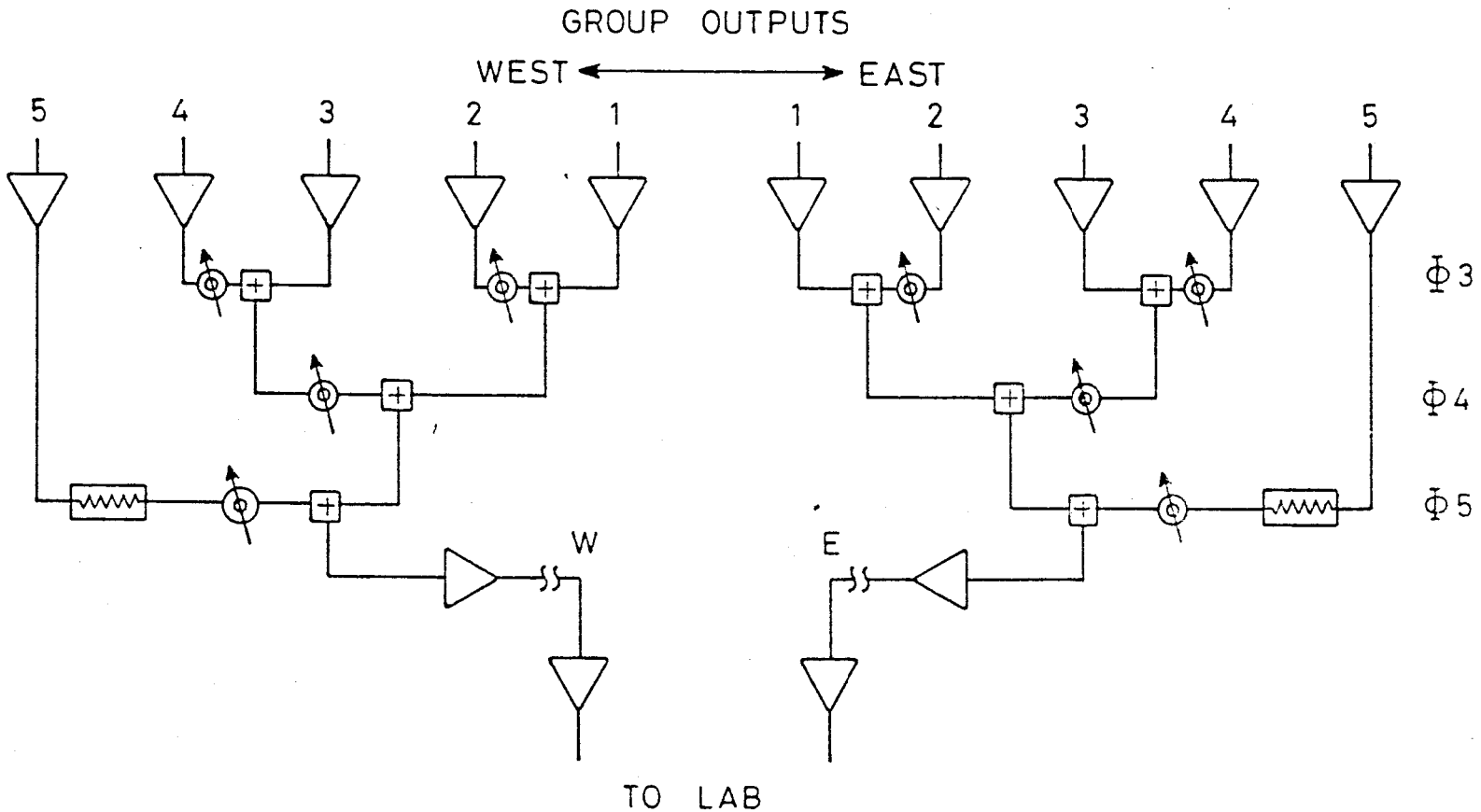

Fig. 2.8 b INTRODUCTION OF NEW PHASE SHIFTERS Φ3, Φ4 & Φ5

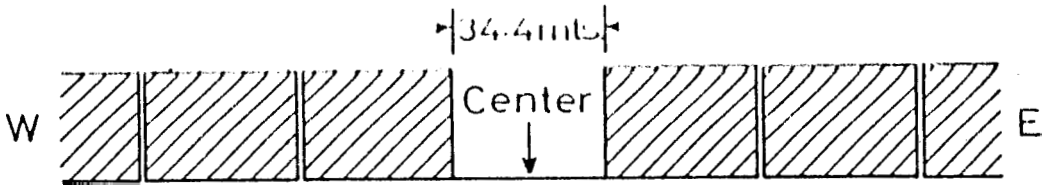

(a) THE APERTURE

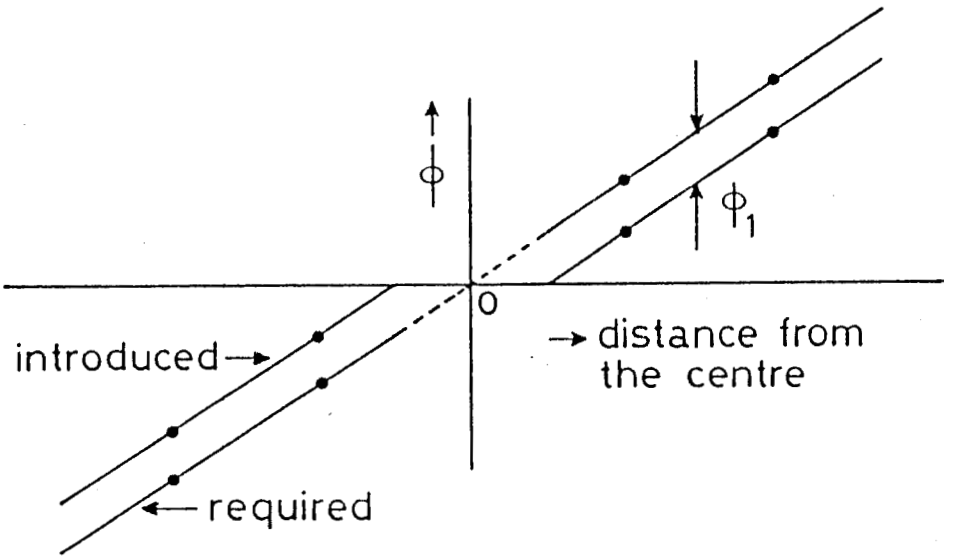

(b) THE PHASE GRADIENTS

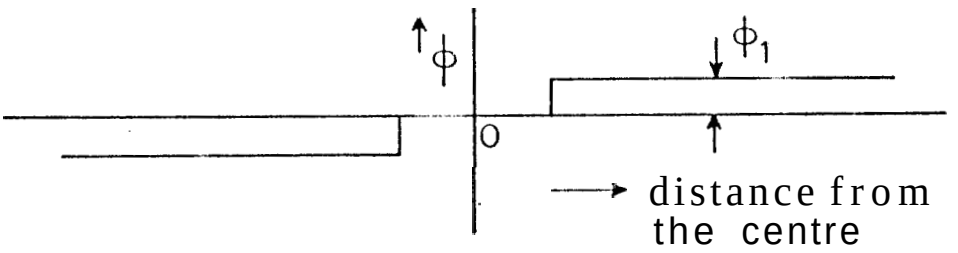

(c) UNCOMPENSATED PHASE

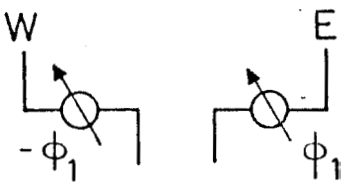

(d) COMPENSATION SCHEME

FIG. 2.9 **Phase gradients and the required compensation.**

and W arms can be phase corrected for the corresponding offsets as indicated in Fig. 2.9d .

2.4.2 Phase Shifters And Pre-amplifiers

As noted in the previous section, we need to install 120 phase shifter modules in the feeder system of the EW array. Fig. 2.10a,b shows the design of a phase shifter module chosen to meet this requirement. Phase shifters of this kind have already been used successfully for tilting the array beams in N-S direction.

This module consist of four sections. Each section consists of two coupled RF diode switches (SW1, SW2). When the control DC voltage is +ve, SW1 is open and SW2 is closed. Thus, the RF signal passes through an additional cable length corresponding to the required phase change. When the control voltage is -ve, SW1 is closed and SW2 is open and the RF signal passes through without the additional phase shift. Each switch consists of two RF diodes. Atleast two diodes are necessary for SW2 in order to isolate the effects of the additional cable length when SW2 is open. And then to make both the paths similar in terms of delay and attenuation, two diodes are used in SW1 also. Using 180°, 90°, 45° and 220.5 phase cables in the four sections and by using suitable control voltages represented by 4 control bits, any phase shift in the range 0 -360^{0} is possible with a maximum error of

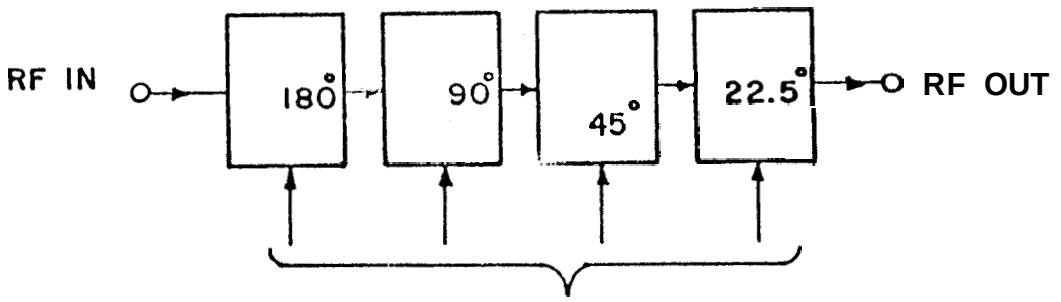

a) FOUR SECTION PHASE SHIFTER

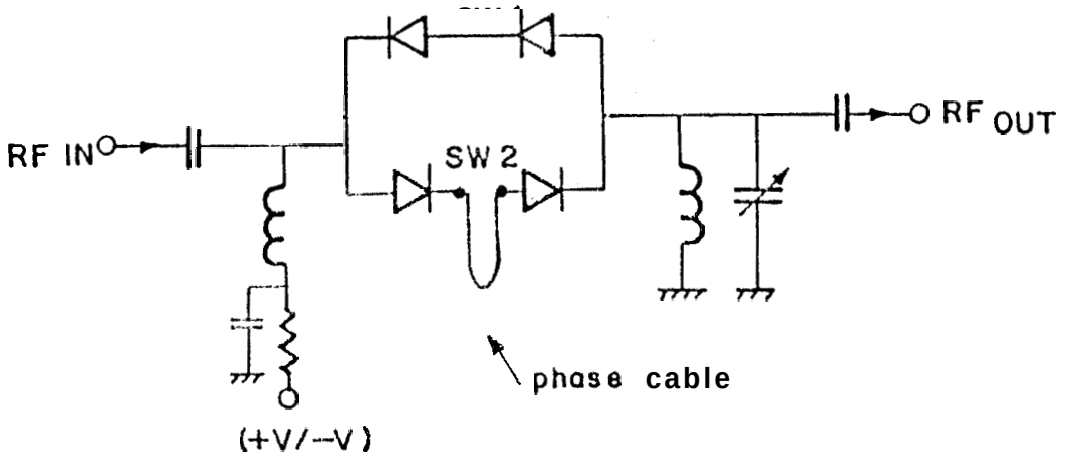

b) INDIVIDUAL SECTION.

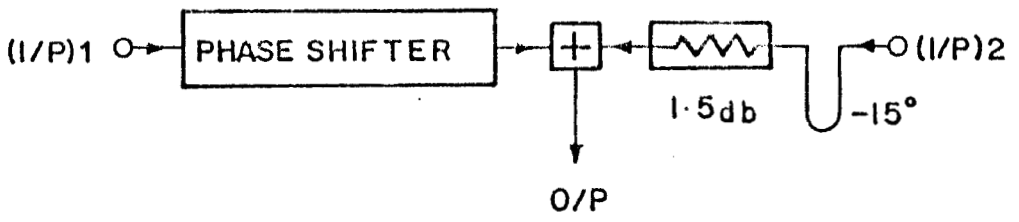

C) PHASE AND ATTENUATION COMPENSATION.

FIG. 2.10 The phase shifter module.

$\pm 11^{\circ}.25$. This phase error would introduce, in general, a random phase error of the same order over the EW aperture and would result in an equivalent r.m.s. beam pointing error of $\sim$ 1.5' arc. As this beam pointing error is very small compared to the beam width in the E-W direction, the least count of $22^{\circ}.5$ is quite acceptable. In practice, the equivalent phase errors and refraction introduced by the ionosphere, at this frequency and latitude, are often larger than the corresponding errors due to the least count of the phase shifters.

The length, L_c, of ϕ° phase cable at 34.5 MHz, if RG174U coaxial cable is used, is given by

$$L_c = \phi^{\circ} \lambda \beta / 360$$
$$= 1.61 \phi^{\circ} \quad \text{cm} \qquad (2.10)$$

where β = velocity factor of the cable
= 0.66 for RG174U cable

λ = wavelength
= 8.71 meters

The response time of this 4 section module is less than 1 msec, The variable capacitors are used to match the input and output impedences to 50 ohms. The module has an average insertion loss of about 1.5 dB and the loss varies by not more than 20.5 dB as a function of the phase shift. The input to output offset phase difference is about -15° at 34.5 MHz.

These phase shifters are to be introduced in the feeder system of the EW array as indicated in Fig. 2.8 . The phase shifter module accepts two array element outputs such that one of them is to be phase shifted and then added to the other. The array element output, which is not be phase shifted, is attenuated by 1.5 dB and phase shifted by -15^{o} and is then added, using a power combiner, to the output of the other array element, which is passed through the phase shifter (Fig. 2.10c). This procedure makes sure that all the basic element outputs suffer on the average the same attenuation and phase shift which is not accounted for by the set phase gradient.

In'the existing EW array, the first amplification is performed at the output of each group of 16 basic array elements. But now we need to introduce two stages of the tracking phase shifters before this stage of amplification. This would attenuate the sky signals by 3 dB more before the first amplifier, and would result in considerable reduction in the signal to noise ratio at the input of the group amplifier. Therefore, we should compensate for this loss, by using additional amplifiers as close to the basic element as possible. We have optimized the number of preamplifiers needed for this purpose and have chosen to introduce a preamplifier after two basic elements have been combined (ref. Fig. 2.11). Thus a total of 80 such preamplifiers were

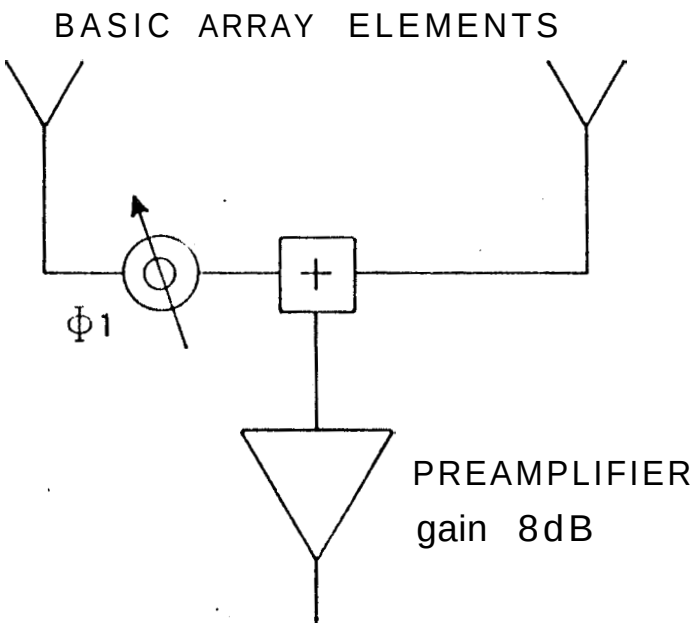

Fig. 2.11 LOCATION OF THE PREAMPLIFIER

installed in the EW array.

2.4.3 *Control* System

For the implementation of the basic scheme discussed in an earlier section, a suitable control system is required to generate appropriate control voltages/signals for the remotely controlled phase shifters at appropriate times. For time-keeping in this tracking operation we require a timing controller which will run according to sidereal time. This timing controller should be able to decide the start and the end times, for the operation over 63 beam positions, depending on the Right-Ascension (RA) and the declination (δ) of a source to be tracked. A source at a declination of 6 takes 40 SEC(δ) sidereal seconds to cross 10' arc of a beam. This time interval corresponds to the observing time in each of the 63 beams, and thus is the time interval between the successive switchings of the beam in the E-W direction. Here onwards we will refer to this time interval as the "beam flipping time" (BFT). For a source in the sky, given its RA and BFT, the start time (ts) and the end time (te) can be expressed as

$$ts = RA - (63/2) \cdot BFT \qquad ...(2.11a)$$
$$te = RA + (63/2) \cdot BFT \qquad ...(2.11b)$$

These times, ts and te, can be calculated using digital counters, where a set of digital counters can be preset to a given value of RA and then (63/2) BFT pulses can be counted DOWN or UP, before reading out ts or te respectively. The worst case error, Δt_q, in such calculations is

$$\Delta t_q = (\Delta RA + 31.5\ \Delta BFT + 1) \text{ seconds} \quad \ldots\ldots(2.12)$$

where $\Delta RA, \Delta BFT$ are the absolute quantization errors in representing RA and BFT respectively.

By using the RA value rounded off to the nearest second and the BFT value to the nearest 0.1 second, this worst case error, Δt_q, can be reduced to 3.075 sec. This error in time will manifest itself in an equivalent beam pointing error of about 0.75' arc in the worst case. As this error is much smaller than the beam size, we need not reduce Δ RA and Δ BFT further. Once the ts and te are calculated, they can be stored .compactly in BCD (Binary Coded Decimal) format in memories of length 20 bits each. In most radio astronomical observations, it is required to obtain an off-source baseline observation in a direction as close to the source as possible. To enable the baseline observations off the source at the same declination and at an earlier but near RA, the EW beam can be positioned at the extreme East direction (31E) of the tracking cone, well before the start time. When the ts becomes equal to the local sidereal time (LST) obtained from the existing Astronomical clock [93], the iracking operation should be

started. At this time, the source will be in the correlation beam at the 95% gain point on the east side. Every BFT seconds after this time the EW beam should be flipped to an adjacent position, 10' arc apart, in the West direction. A set of counters can be used to count for BFT seconds and to generate a 'flip' pulse after each end of BFT seconds starting from the start time . These 'flip' pulses can be used to clock a "beam counter" with 63 (31E, 30E . . . 2E, 0, 1W,2W . . . . 30W, 31W) stages. A simplified block diagram of this timing controller is shown in Fig. 2.12 . The 6-bit binary output of this counter can be used to obtain appropriate control signals for the tracking phase shifters. Thus, by using this 6-bit information (B5--> B0), we have to generate 40 bits of information to control the phase shifters.

The most significant bit of these 6 bits tells us whether the beam position is on the East or West of the meridian. Therefore, the remaining 5 bits are to be used to produce 5 sets (ϕ1--> ϕ5) of 4 control bits each. It should be noted, that the phase shifts required at various stages have the following binary relationship.

$$2^{(5-i)}\ \phi i = \phi 5 \qquad \text{....(2.13)}$$

for $i = 1,2,\ldots,5$

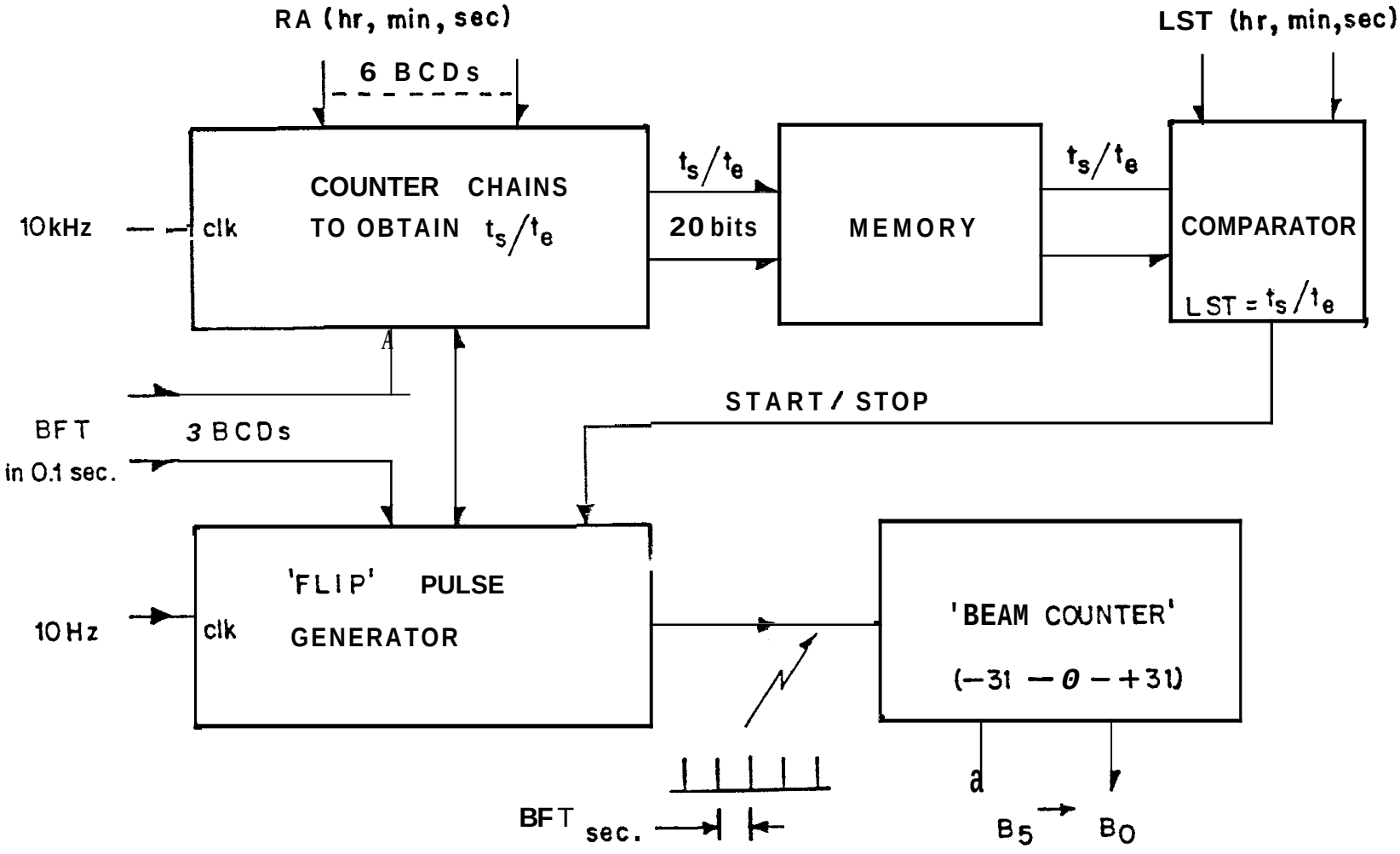

FIG.2.12 Block diagram of the timing Cantroller.

Further, ϕi itself is represented, to an accuracy of $\pm 11.25^{\circ}$, as a 4-bit binary number which is modulo 360° and can be expressed as

$$\phi i = 22.5^{\circ} \sum_{4}^{j=1} 2^{(4-j)} \, Cji \qquad \ldots(2.14)$$

where Cji = 1 or 0

= 1-bit control signals for phase shift $(360/2^{j})^{\circ}$

and $i = 1,2,\ldots,5$

Using the 5 bits (B4--> B0), if we can generate a 8-bit binary number (b1,b2,....,b7,b8) corresponding to $\phi 1$, then by using the above properties of ϕ, we can subsequently obtain the 4-bit representations for all the five stages (i= 1--> 5) as shown in Fig. 2.13. Thus the problem, is now reduced to generating these 8 bits from the 5 bits (B4--> B0) of the counter output. The phase shift $\phi 1$ for the East arm when the beam is in the n_bth ($0 \leq n_b < 31$) position on the East is given by

$$\phi 1 = [-360 \, d1 \, SIN((n_b/6)^{\circ}) / \lambda] \qquad \ldots.(2.15)$$

where d1 = distance between two basic array elements in E-W direction

= 34.N meters

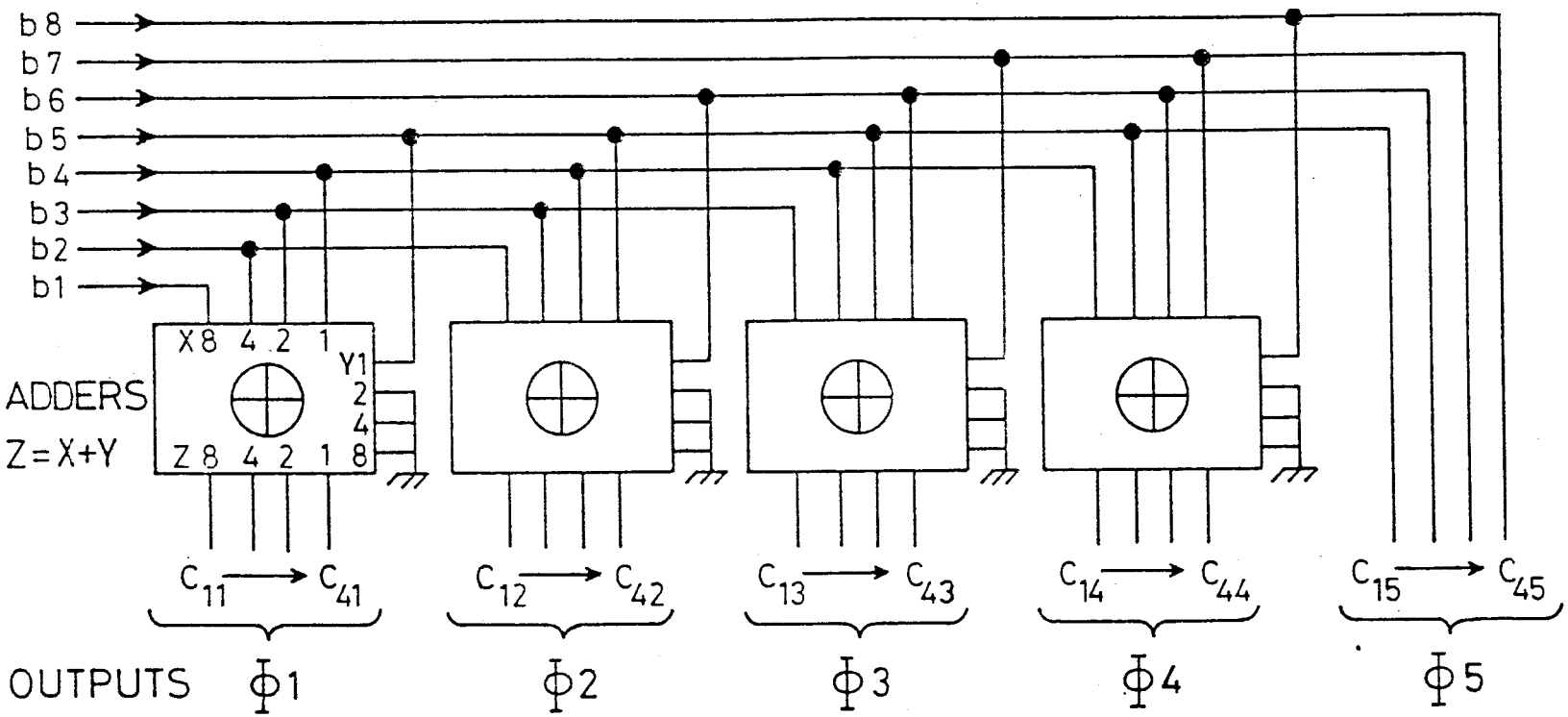

FIG. 2.13 A scheme to obtain 4-bit representations for $\phi 1 - \phi 5$

For each value of n_b, the corresponding 8-bit representations can be computed for values of $\phi 1$ given by the above equation. Each of these 8 bits for $\phi 1$ can be generated with the 5 input bits (B4--> B0) using suitable combinational circuits.

As noted in the earlier section (ref. eq. 2.8), the phase shifts required for the West arm are equal, but opposite in sign, to those for the East arm. Therefore the control sets generated for the East arm can be two's complimented and used as the control sets for the West arm phase shifters. In this manner, we are able to produce the required 40 control bits which will produce appropriate tracking beams on the East of the meridian. Now by interchanging the control sets for the East and West arms (ref. eq. 2.8), we can produce symmetrically placed EW beam on the West of the meridian. A block diagram of the scheme to generate all the required control sets from the 6-bit (B5--> B0) output of the "beam counter" is given in Fig. 2.14 .

The control system, which consists of the timing controller and the control sets generator described here, has been built using CMOS integrated circuits. The CMOS devices were chosen noting their lesser power requirement and higher noise margin compared to those of other device types.

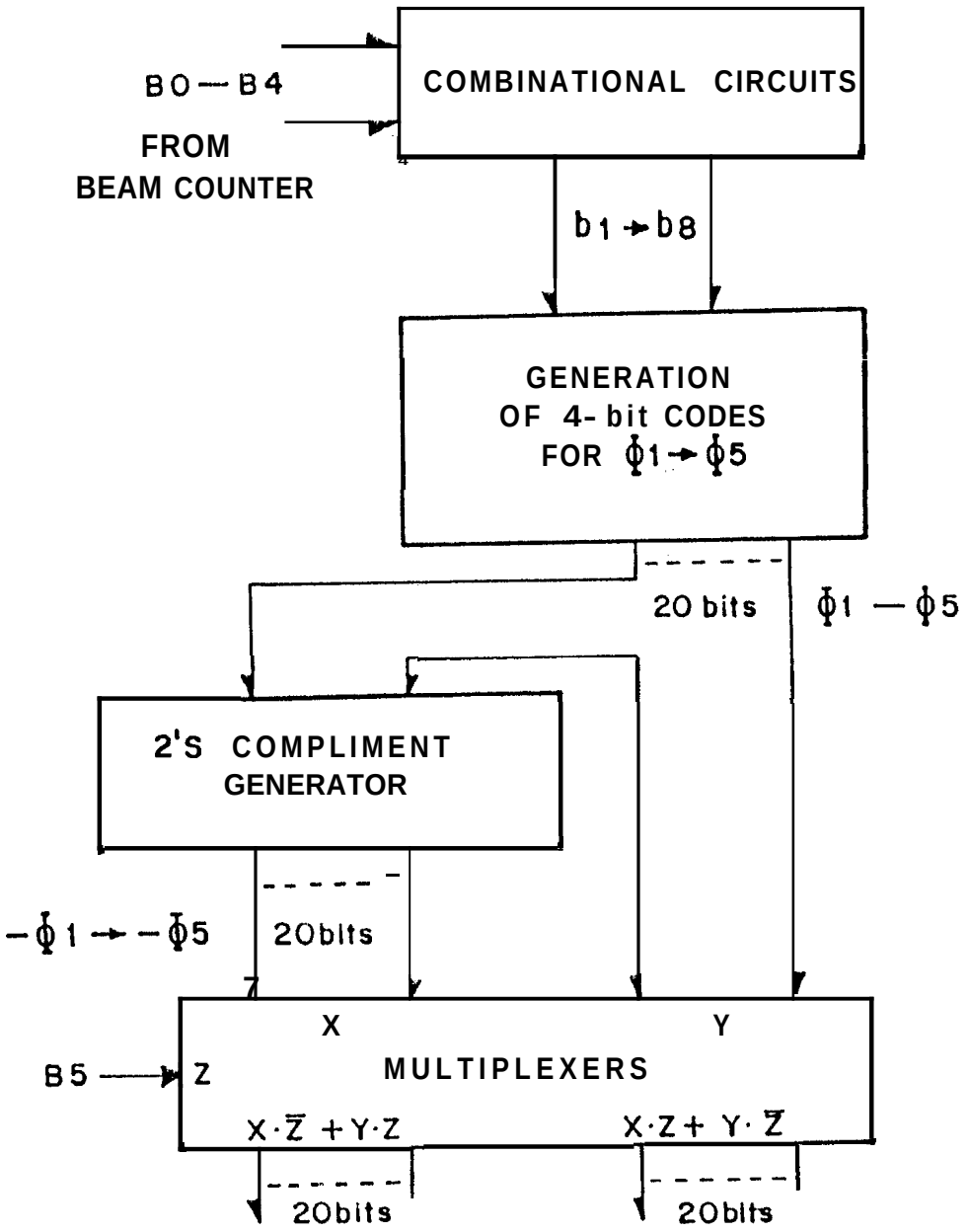

FIG. 2.14 Generution of all the required control sets from the output of the Beam Counter.

2.4.4 Driver/Display For The Control Signals

The control signals generated in the control system are CMOS outputs with 0 to 5 Volts swing. These CMOS outputs need to be converted into suitable bipolar outputs to drive the phase shifters with appropriate DC currents. Suitable driver modules to enable this conversion have been built. The circuit diagram of this module is shown in Fig. 2.15 . The CMOS output signal from the control system is first level converted to ±12 Volts peak-to-peak, using an operational amplifier (OPAMP) in its open loop configuration. This opamp output is then used to operate two transistor-switches (SW1,SW2). The output ends of these two switches (i.e. the emitters) are shorted and are inturn connected to the phase shifter control inputs in the field through open wire transmission lines. This configuration is designed to produce a DC voltage of 6 Volts with appropriate polarity across the field load. In each collector path a Light Emitting Diode (LED) indicator is provided with a series resistance (R1). Depending on the field load ,a parallel resistance (R2) is provided such that the parallel combination of R1 with R2 approximately matches the field load.The field load resistance is inversely proportional to the number of phase shifters which receive the corresponding control signal. The minimum value of R1 is restricted considering the maximum current that can be safely passed through the LED. The two colours for the

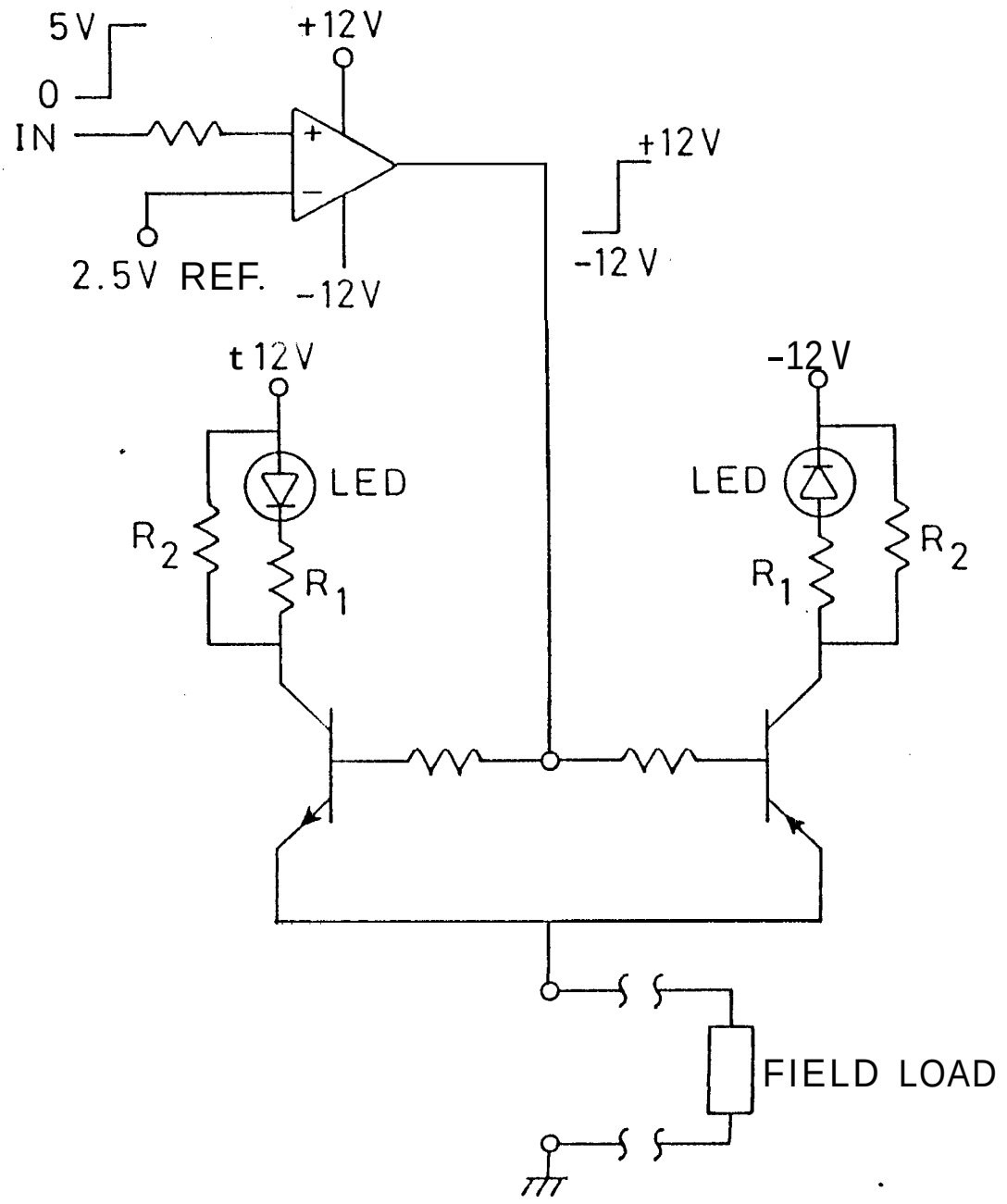

FIG. 2.15 The driver/ display module : circuit diagram.

LEDs give an indication of the polarity of the control voltage sent to the field. If both the LEDs fail to glow, it indicates absence of the field load.

2.4.5 Performance Of The Tracking System

The tracking facility has been built following the design aspects discussed in the earlier sections and installed successfully after appropriate testing. Fig. 2.16 shows an observation made on a point source (angular size of the source << beamwidth) using the tracking facility in the (EW)X(S) correlation mode. This example amply demonstrates the satisfactory operation of the tracking system.

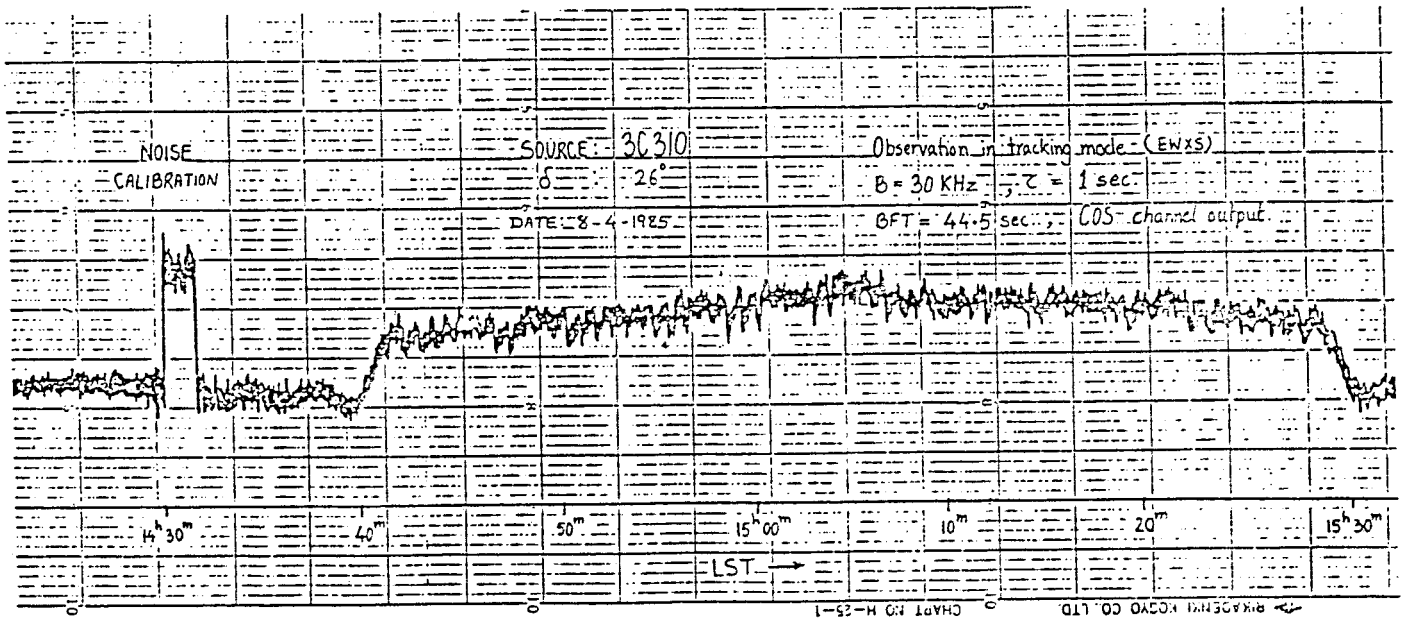

FIG. 2.16 A point source observation with the tracking system.